TRACE EXTRACTION FROM OBLIQUE IONOGRAMS.

Applied MAchine Vision, '96, Cincinnati, Ohio, USA, 1996

Matthew Roughan

July 9, 2003

1 Introduction

Oblique sounding may be used to obtain information about the ionosphere, in the form of an electron density profile, near the mid-point of two sites. This makes it useful for recovering ionospheric data at a point at which, for reasons of economy or geography, vertical sounding cannot be conducted. The information may be used in providing real-time propagation advice either for over-the-horizon radar, or high frequency (HF) communication.

A HF signal is transmitted obliquely through the ionosphere. The signal refracts through the ionosphere following a path such as that shown in Figure 1, to the receiver site. The frequency of the signal is swept through some range so that the received power can be recorded both as a function of transmission frequency and group range (the length of the path traversed by the signal). This produces an *oblique ionogram* an example of which can be seen in Figure 2 which shows a ionogram from the frequency management system (FMS) of the Jindalee over-the-horizon radar program at Alice Springs, Australia [1].

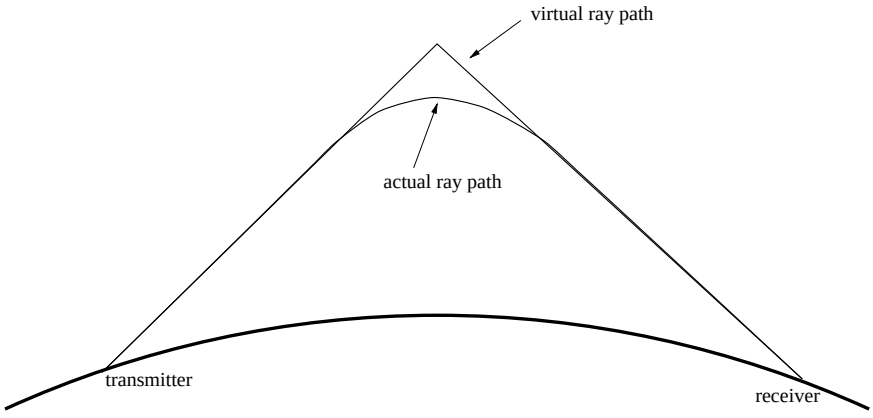

Figure 1: Transmission of a signal through the ionosphere. As shown in the figure the actual ray path is produced by refraction, not reflection as in the virtual path.

The ionogram contains *traces* which correspond to physical modes of transmission through the ionosphere. The common modes correspond to the E, F1 and F2 layers of the ionosphere, while there are also complex modes resulting from refraction from several layers, and scattering from the ground. (For further information on the ionosphere see Davies [2].) Figure 3 shows the traces that are present in the ionogram shown in Figure 2. The shape of the traces is dictated by the ionospheric conditions and can thus be used to recover information about the ionosphere through inversion [13, 16]. In order to use the information contained in the

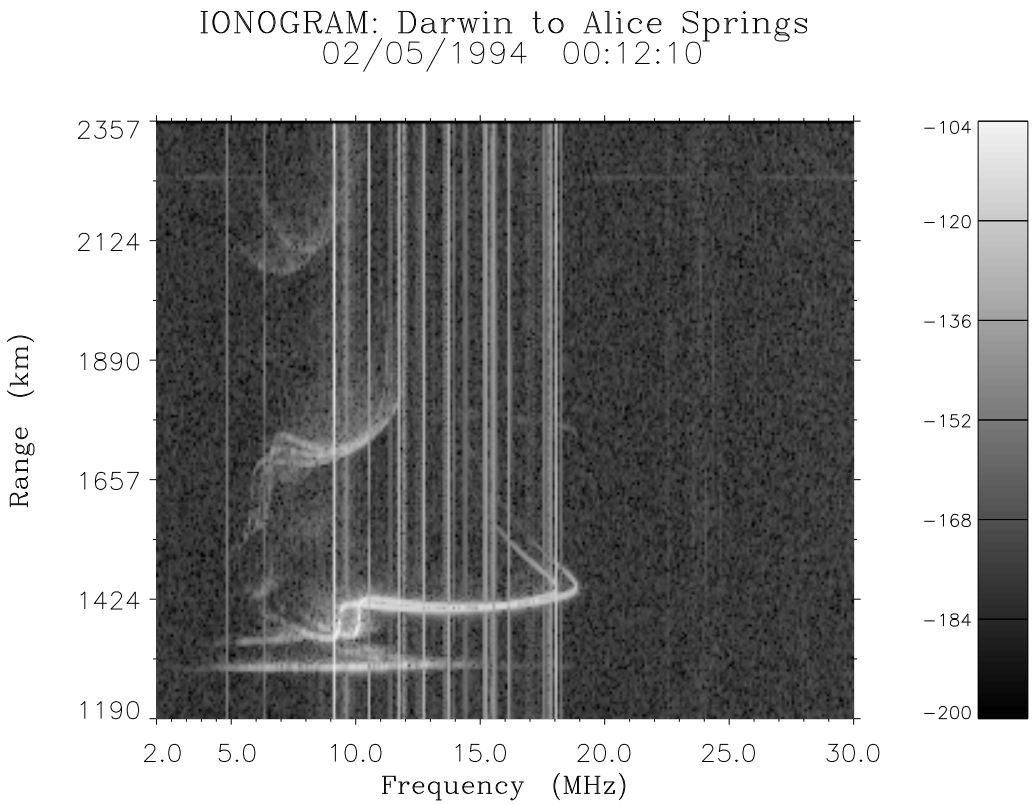

Figure 2: A raw FMS ionogram. The scale on the right shows received power in dBW.

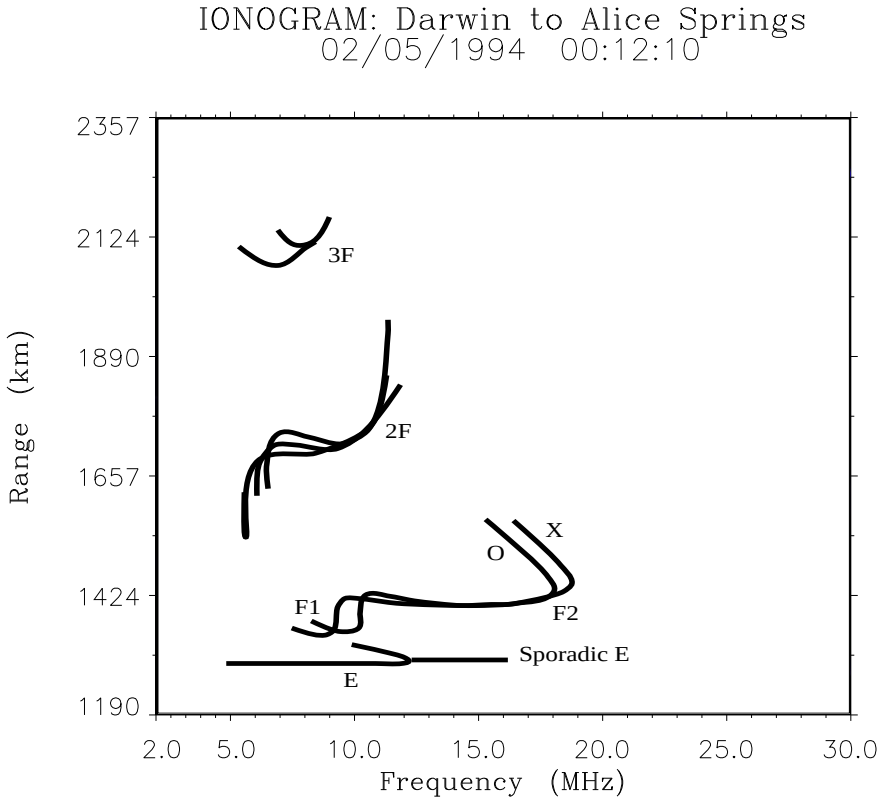

Figure 3: The ideal result of trace extraction. Each ionospheric trace is shown labelled by its corresponding ionospheric layer, and mode of propagation. The 2F and 3F layer traces denote traces caused by second and third hops off the F-layer of the ionosphere.

ionogram the traces must be extracted. Thus reliable, automatic extraction of traces is a central problem in the provision of real-time HF propagation advice.

The extraction of traces resembles other problems in computer vision, in that it involves extracting curves to represent objects in an image. As in many such tasks, it is relatively easy for a human operator, but would require a prohibitive amount of human time to perform. This report presents a method for *automatic trace extraction* primarily using computer-vision techniques.

The problem of reliable trace extraction is a difficult one. Typically until now only vertical-incidence ionograms have been collected regularly because techniques for trace extraction from such have been developed, for instance [5, 8, 17]. The variety of trace shapes in oblique sounding due to different ionospheric conditions, base-lines and ionospheric gradients, adds an order of difficulty to the problem, and there seems to be as yet little work published in the open literature on the problem.

A further problem is that the oblique ionograms in question contain only amplitude information. In vertical sounding there is typically considerable extra information available such as polarization information, Doppler, and information about the angle of arrival of received signals. Polarization information in particular would make the task easier, but is harder to gather in oblique sounding.

Figure 2 shows a FMS oblique ionogram, a 280x240 pixel gray-scale image, with image values representing

received power. This ionogram shall be used to demonstrate the algorithm within this report. The ionosphere varies on a diurnal, seasonal and 11 year basis, and so it is impossible to present a typical ionogram, but the one displayed in Figure 2 demonstrates the algorithm well, while an objective assessment of the algorithms performance is presented in Section 3.

The approach adopted herein is to use image processing techniques to (i) remove noise from the ionograms and (ii) extract the traces. Part (i) can be very successfully accomplished, while an algorithm for (ii) has been developed though it is still in the experimental stages. Though the ideal result of trace extraction is shown in Figure 3, the principle requirement for the algorithm is to produce a trace which can be used in the inversion procedure. It is overly optimistic to expect an automatic algorithm to produce all of the traces (particularly multi-mode traces) and so this paper concentrates on extracting the traces corresponding to a single hop from the F2 layer (or simply the F layer when the F1 and F2 layers are not split) and in conjunction with this, separating the *x*- and *o*-modes of transmission. The F2-layer trace (with polarization separation) is the primary requirement for an inversion procedure as the F1- and E-layers of the ionosphere are amenable to simple modelling.

This report is organised as follows. Section 1.1 details some of the specific problems with the FMS data, and oblique ionograms in general. The algorithm is designed specifically to combat the difficulties presented by the data. Section 2 describes the algorithm. The algorithm has four basic parts. The first is preprocessing to remove noise, discussed in Section 2.1. The next two stages find a set of possible traces, firstly finding approximations to the traces and then refining the approximations, in conjunction with separating the two polarization modes, described in Sections 2.2 and 2.3 respectively. The two stage process is used primarily to reduce the computation time of the algorithm. Finally the possible traces are classified to provide a single trace corresponding to the F2-layer in Section 2.4. Section 3 discusses the algorithm's performance.

1.1 Problems

There are considerable problems associated with designing a trace extraction algorithm for the FMS ionograms. These stem from the desire to have a *robust* algorithm, despite noise and the variability encountered in the set of ionograms. The variability makes simple techniques such as template matching or the generalised Hough transform quite untenable.

It will serve the reader well to know a little about the major difficulties faced in the trace extraction problem. The major problems are therefore listed below with some discussion of each.

Blanketing: Strong sporadic-E may reflect all HF radiation, *blanketing* the rest of the ionosphere. This can cause the F-layer trace to be very weak, or completely missing. In cases where the F-layer trace is missing, blanketing can only be detected by examining a sequence of ionograms.

Instrumental effects: The instruments used to transmit and receive the signals are not perfect and can introduce effects. A typical such effect in the FMS appears as horizontal lines in the ionogram.

Night-time: During the night the ionosphere may become so reduced that its appearance on an oblique ionogram is negligible.

Overlapping traces: Traces may overlap. The *x*- and *o*-modes of transmission overlay each other, possibly in a very complex fashion, making their separation difficult. Multiple real traces often overlay each other while traces from multi-hop paths or multi-modal paths can also overlap the trace of interest. This is a very serious problem.

Radio frequency interference: Radio frequency interference (RFI) is of major importance in ionograms. RFI appears as vertical lines in an ionogram. When strong RFI occurs, particularly around the critical frequency of a trace it can make accurate assessment of the trace impossible.

Spreading: Spread F, in both frequency and range can cause great problems even for a human operator. Spread is exactly what it sounds like, a spreading of the traces. Strong spread can make an accurate determination of the trace impossible.

Travelling ionospheric disturbances: A travelling ionospheric disturbance (TID) may distort the trace considerably making shape based approaches to trace classification difficult. To properly detect such disturbances temporal information must be used.

In some ionograms several of the above phenomena occur, or problems occur which cannot easily be explained by physical effects making an ionogram very difficult to analyse. These problems make 100% trace extraction impossible, even for a human observer. Some of these phenomena, such as RFI, may be combated successfully via strategies adopted in this algorithm, however others, such as spread and TIDs, must be identified and flagged in order to provide some measure for the accuracy of the algorithm. This has not as yet been accomplished due to the difficulty of the task, for instance, to classify a TID or blanketing, information derived from a sequence of ionograms is required.

A more general problem with the analysis of oblique ionograms is the absence of an analytic model for the shape of the traces. Serious ionospheric models for oblique transmission all use ray-tracing through a complex model to synthesise ionospheric transmission. Thus a non-parametric approach to trace extraction has been used herein.

2 The algorithm

2.1 Preprocessing

The preprocessing of an ionogram is an important stage. Ionograms contain several forms of noise which must be removed before the main part of the algorithm can commence. The preprocessing adopted in this algorithm is described below.

The most visible form of noise in ionograms is radio frequency interference (RFI) which appears in an ionogram as vertical lines. Several techniques for removing RFI have been suggested, for instance Fourier filtering in Hazelwood [7] and an artificial neural network method in Koschmieder [12]. A number of such methods have been tested on the FMS database with the most useful being an adaptive threshold chosen independently for each frequency. An example of the RFI removal algorithm applied to an ionogram is shown in Figure 4.

The main layer of interest in this paper is the F-layer. The E-layer merely complicates the image and so its corresponding trace is removed. The E-layer occurs within certain height limits in the atmosphere (90-120 km), and hence in an ionogram appears as a nearly horizontal trace. A profile based segmentation routine is used to remove the E-layer traces. A vertical profile of the ionogram is formed by finding the mean value of the ionogram in each group range bin. By examining the profile, significant horizontal lines (such as the E-layer trace) may be found and eliminated. A heuristic is used to decide which horizontal lines are significant enough to remove. Unfortunately it is impossible, in general, to remove all of the multiple-hop E-layer traces, as they may overlap the F-layer traces, but this is not critical at this stage.

Removal of RFI can have the deleterious effect of removing parts of the traces when the RFI is intense (see Figure 4). Furthermore the trace is not a smooth curve as may be desired. Both of these problems can to some degree be mitigated by using a morphological filter. In this case a gray-scale mathematical-morphological closure with a three by three structuring element is used, this being equivalent to a local maximum operation (dilation), followed by a local minimum operation (erosion). This filtration will bridge small gaps (1 or 2 pixels wide) in the trace and simultaneously smooth the trace. Other methods of filtering, for smoothing purposes do not have such beneficial effects when it comes to bridging gaps.

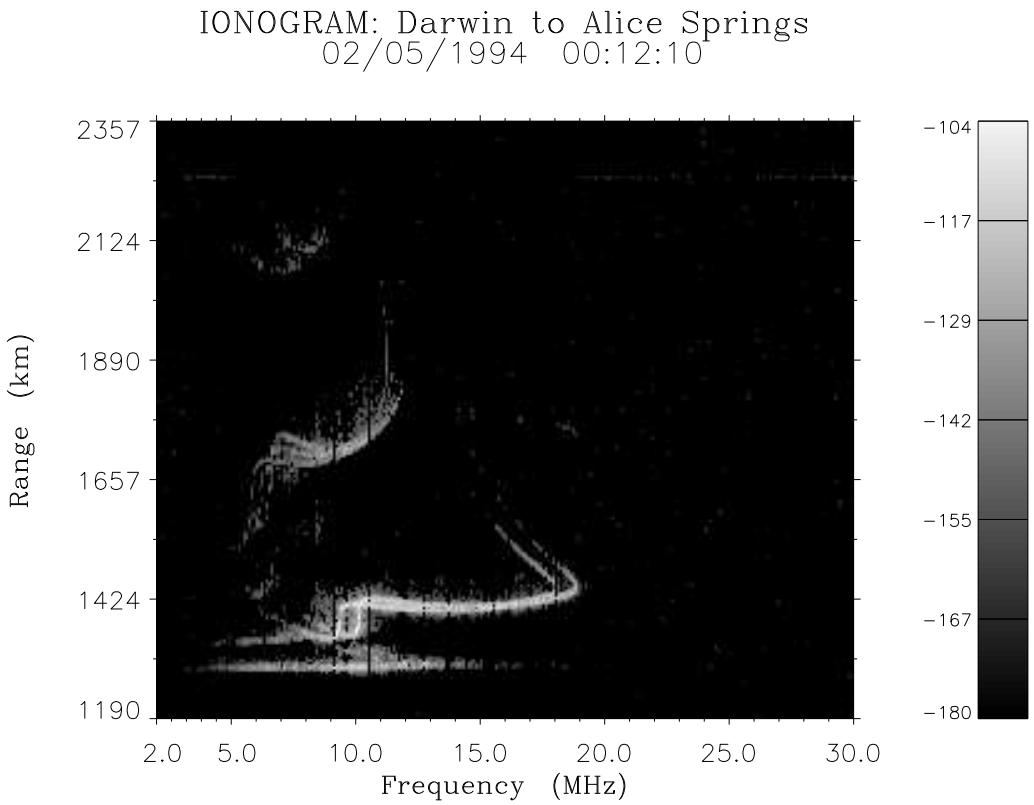

Figure 4: An ionogram with the RFI removed. Note the gaps in the trace at 9 and 10.5 MHz, where strong RFI caused part of the trace to be removed as well.

A further morphological filter is then applied to enhance ridges. The operator is called the morphological skeleton [15]. It consists of the sum of the image successively eroded and transformed by the top-hat transformation. The top-hat transformation can be written in morphological notation as

$$f - (f \circ B).$$

$f \circ B$ is the opening of the image f by the structuring element B. Repeated application to erosions of the original gives the morphological skeleton,

$$SK(f) = \sum_{n=0}^{N} \Big[(f \ominus nB) - [(f \ominus nB) \circ B] \Big],$$

where in this case N was chosen to be 4.

After RFI removal and the other filtering operations, there is still some noise in the ionogram, commonly appearing as isolated, or nearly isolated points. There are many techniques for removing noise (see [11, pp 65]) some of which have been tried in Redding [**?**] but a different technique, an area-based thresholding, is used here, suggested by the isolated nature of the noise.

Connected regions are found using an algorithm based on Haralick and Shapiro [6]. The algorithm uses two raster passes through the ionogram to label each 8-connected region uniquely. Two points are said to be 8-connected if one lies in any of the eight immediately adjacent pixels of the other or if there is a third pixel

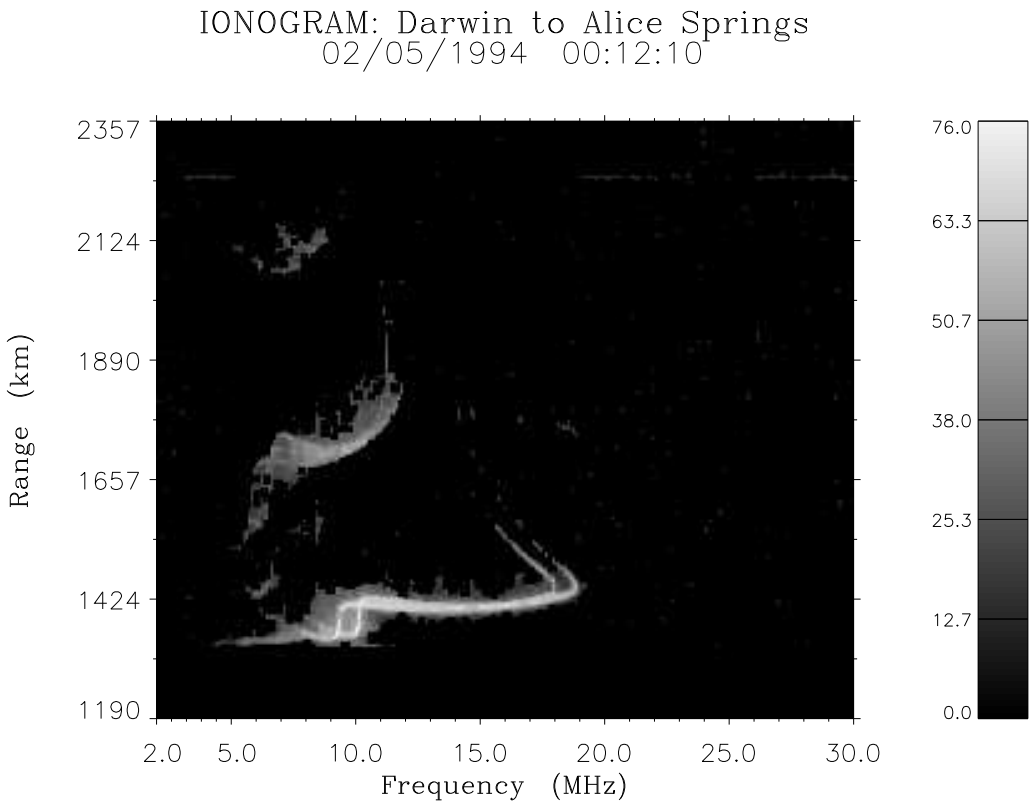

Figure 5: A morphological closure (by a 3x3 structuring element) of the ionogram once RFI and the E-layer trace are removed.

which is 8-connected to both pixels. If each point in a region is 8-connected to all other points in the region then the region is said to be 8-connected.

The result of the algorithm is that each non-zero point on the initial image is given a label corresponding to the unique label of the region to which it belongs. The areas of these regions (in pixels) are then computed by again passing through the array, and simply counting the occurrence of each label. Regions with an area greater than a threshold are retained while other regions are discarded.

An adaptive threshold has been chosen by considering a histogram of the square roots of the areas of regions in the image. The threshold is set where this histogram first drops to zero. This removes the majority of noise with minimal degradation of traces.

The final result of the preprocessing is then the smoothed ionogram, masked by the regions remaining after area-thresholding the top-hat transformed, smoothed ionogram. This result is shown in Figure 6. Note though that the data from each of the preprocessing steps is not discarded, and may be used in later stages of the algorithm.

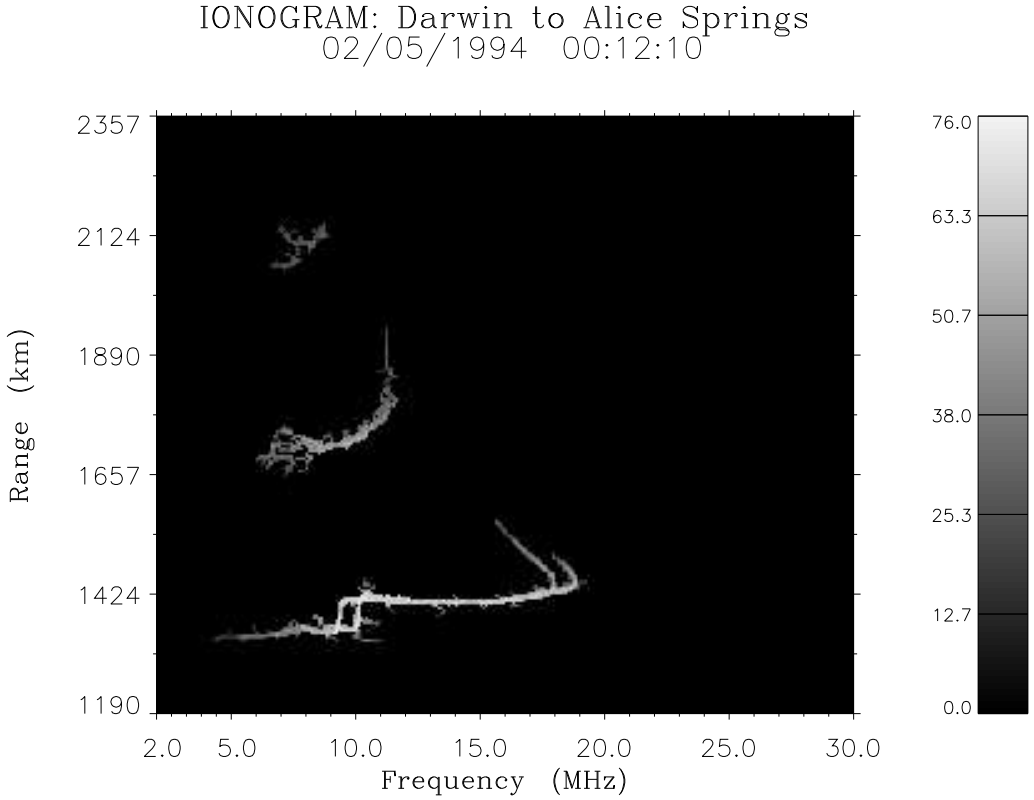

Figure 6: A preprocessed ionogram.

2.2 Preliminary trace extraction

Once the ionogram is preprocessed a two stage processing system is used to extract possible traces. The first stage is similar to a preattentive stage, designed to identify candidate traces and approximate them. The second stage refines each approximate trace, and separates the two polarization modes. The principle advantage of the two stage approach is that the more computationally intensive parts of the algorithm can be restricted in focus to a specific region of the ionogram, greatly increasing performance.

Several skeletonisation techniques were trialled for the first stage, referred to here as preliminary trace extraction, but these suffered from noise branching problems. The preliminary trace approximations do not need to be extremely accurate, and in fact, the lower-ray part of the trace is quite sufficient, so a different method for extracting trace approximations has been used. The method used is tracking along the ridges of the traces from a set of starting points. This can be thought of as a novel way of finding the skeleton of the trace. The advantage of tracking over most other forms of skeletonisation is that tracking is less sensitive to noise, and can simultaneously smooth the trace approximation. Furthermore tracking can jump small gaps in a trace, left by the RFI removal algorithm, or partial blanketing. The major limitation of tracking (that it can only find a single curve for each starting point) does not impact on this algorithm, as only a single curve is needed to represent each trace.

2.2.1 Tracking

The points from which tracking commences, the starting points, are selected by considering each connected region separately. Each region is placed upon a rectangular grid, and in each rectangle of the grid one starting point is chosen at the maximum pixel-value within that rectangle. If two or more starting points are adjacent then only one is allowed. In this way a good distribution of starting points over the entire region is obtained. It is more important here to make sure that the F2-layer trace will be found than to prevent false detection, and so the grid size was chosen conservatively at 40x20 pixels. In the example considered 16 starting points were found.

The tracking algorithm selected was the Kalman filter, the dominant algorithm for tracking. The Kalman filter [19] is, simply speaking, a method for estimating the mean and covariance of a set of vectors in some linear dynamic model in the presence of white Gaussian noise.

$$x_{n+1} = Fx_n + Gv_n, \tag{1}$$

where the sequence of column vectors $\{x_n\}$ are the system state at time n and $\{v_n\}$ is an i.i.d. sequence of zero-mean Gaussian-distributed random variables (or white Gaussian noise). $\{v_n\}$ is called here the system noise. The values x_n cannot be measured directly but must rather be estimated from a measurement,

$$z_n = Hx_n + w_n, \tag{2}$$

where $\{z_n\}$ is the measurement process and $\{w_n\}$ is the measurement or observation noise, again an i.i.d. sequence of zero-mean Gaussian random variables. For this model the Kalman filter is an optimal method (in a least squares sense) for estimating the x_n.

The Kalman filtering equations (see [19]) based on the above model provide a simple recursive procedure for performing the estimation. As an initial condition, x_0 is assumed to be a Gaussian random variable of known mean $\overline{x}_0$, and covariance P_0, independent of $\{v_k\}$ and $\{w_k\}$.

In general Q, R, F, G, H may all depend on n but this is unnecessary for the application herein. Note also that the actual values of Q and R that are used in estimation may not be those actually specified by the real noise in the model. The values may be chosen to achieve certain aims such as smooth results. This results in a sub-optimal implementation but may obtain better results in a sense other than minimum least-squared errors.

Because the Kalman filter estimates a linear system, and the traces in question are decidedly non-linear the implementation of the Kalman filter is sub-optimal. There are better approaches to a non-linear problem such as the extended Kalman filter or hidden Markov models. These have not yet been trialled as the standard Kalman filter performs adequately.

The Kalman filter is applied by considering the trace to be a function of frequency (the x-axis of the plot). Thus frequency plays the part of time in a standard tracking application. This restricts the trace approximations in that they cannot encompass the curve around the nose region of the trace, but this is not a problem for the initial trace approximations, as they need only approximate the lower ray of the trace. The resultant trace approximations are very robust even in the presence of heavy spread, overlapping traces or a TID. The only way in which the limitations of a 1D tracker can cause problems is if there is no significant lower-ray trace. This happens in daytime ionograms, during blanketing and occasionally during night-time ionograms, but in these cases very little can be done without considering a sequence of ionograms.

The dynamic model used is given by equations 1 and 2, where the state $x_n = (range, slope)^T$, n refers to the frequency and

$$F = \begin{pmatrix} 1 & 1 \\ 0 & 1 \end{pmatrix}, \quad G = \begin{pmatrix} 0 & 0 \\ 0 & 1 \end{pmatrix}, \quad H = (1\ \ 0).$$

The track is initiated at a starting point and continues both to the left and to the right. The starting slope is assumed to be zero. Thus if the starting point is the pixel (x, y) of the ionogram then $x_0 = (x, 0)^T$. The

track terminates when it has traversed gap a maximum of 0.3 MHz wide (where the frequency resolution of the FMS ionograms is 0.1 MHz).

The measurements of the new position is taken by finding the maximum pixel value in a window around the predicted value. The window size was chosen empirically but a more acceptable method for choosing the window would be to use a probabilistic data associating (PDA) Kalman filter which would automatically select a measurement gate, and thus eliminate these parameters. In addition a PDA Kalman filter would allow a less arbitrary method for crossing gaps, as it allows for missing data. Further the termination criteria could be weighted by pixel intensity rather than having a fixed threshold. A PDA Kalman filter has not yet been implemented as other parts of the trace extraction have received priority but is high on the list of future improvements.

2.2.2 Preliminary classification

Once the tracks have been found, it may be noted that several are either redundant, or cannot possible be an F-layer trace. Thus, motivated by a desire to reduce the number traces which are examined in later phases, some preliminary classification on the trace approximations is done. The number of traces to be examined can be substantially reduced without a significant chance of removing the F2-layer trace.

The first classification actually occurs during the tracking algorithm. Tracks less than 15 pixels (1.5 MHz) in length are discarded. Even if one of these does correspond to a real trace, a track of this length is not much use for anything further. Only 6 tracks rather were found in the example rather than one for each of the 16 starting points.

Next, redundant tracks returned by the Kalman filter are removed. There will be many either identical, or very similar tracks because more starting points have been used than there are traces in the ionogram. To remove the extra tracks they are *associated*. Two associated tracks are assumed to correspond to the same trace, and so one track can be removed. The decision to associate a pair of tracks is made by considering how much the two tracks overlap. If the longest contiguous segments of the tracks is greater than 1.5 MHz and the longest discontiguous segment is less than 3.0 MHz then the two tracks are associated. Once two tracks are associated one must be removed. Rather than simply remove one track, the best parts of both tracks are kept. The summed brightness of pixels along each discontiguous segment of the two tracks is considered and the brighter segment is retained. In the example, 6 tracks were reduced to the 2 tracks.

There are sometimes included in our list, tracks produced by instrumental effects in the FMS. These appear as horizontal lines at relatively high group ranges. Tracks produced by the F-layer must be within certain group ranges. Thus by eliminating any straight line tracks which would correspond to traces above 600km in virtual height, we remove the effect without effecting the traces of interest.

The tracks left may still have shapes which would disallow them as possible F-layer lower-ray traces. A heuristic (based on the slope of the trace) has been chosen to eliminate traces (or sections thereof) which cannot be part of an F-layer lower-ray trace. The heuristic is quite conservative, in that it will allow quite a range of shapes through to later stages.

Figure 7 shows the tracks found by the algorithm, once reduced in number to two by the elimination of impossible tracks. The two tracks follow quite closely the *lower-ray* trace of the F2-layer, and the 2F-layer trace.

Finally the traces are classified purely by their remaining length, assigning to each a notional probability proportional to the exponential of the horizontal length of the trace. This form of probability can be justified on the basis of the maximum entropy principal, or other probabilistic arguments, but it can easily be seen why this form of probability is useful:
(1) a set of lines with many short lines and one long line will still assign a large probability to the long line.
(2) two similar length lines will be assigned similar probabilities.

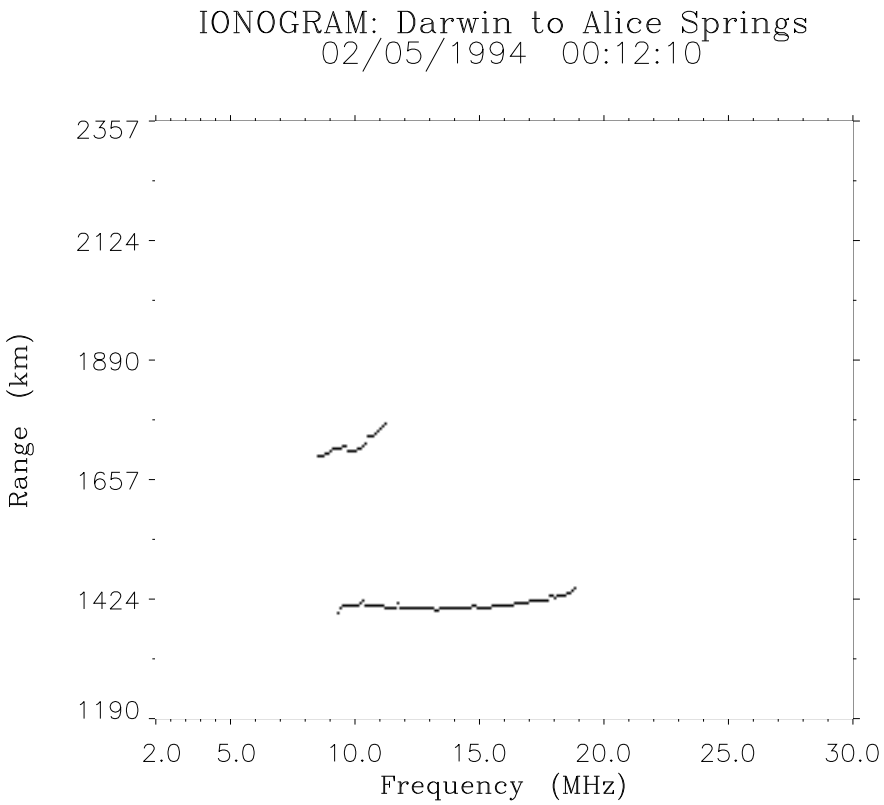

Figure 7: The tracks found by the algorithm, once shape based classification has taken place.

Any trace approximation assigned a probability of less than 0.1 is eliminated from further consideration. This often leaves just one trace and rarely leave more than two. (Sometimes previous classification stages can eliminate all traces, in which case there is nothing more to be done.) As an example the upper and lower trace approximations in Figure 7 are given probabilities 0.03 and 0.97 respectively. Thus only the lower track is investigated further.

2.3 Mode identification and trace extraction

Once an initial approximation to a trace is found attention is restricted to a region around these traces. Each of the traces provided by the previous phase is treated separately and only a small rectangle, called here the region of focus (ROF), is investigated for each trace. This speeds up computation and also excludes extraneous data from consideration. Thus ideally the region would be as small as possible, excluding all such extraneous data, but containing all of the relevant data. A adaptive routine has been designed to select the ROF so as to fit these criteria as closely as possible. An example of a region of focus around a trace is shown in Figure 8.

The next step will be to Hough transform the ROF to detect the *upper-ray* traces. Preprocessing of the ROF may reduce the computational load of the Hough transform as the load is directly proportional to the number of points to be transformed.

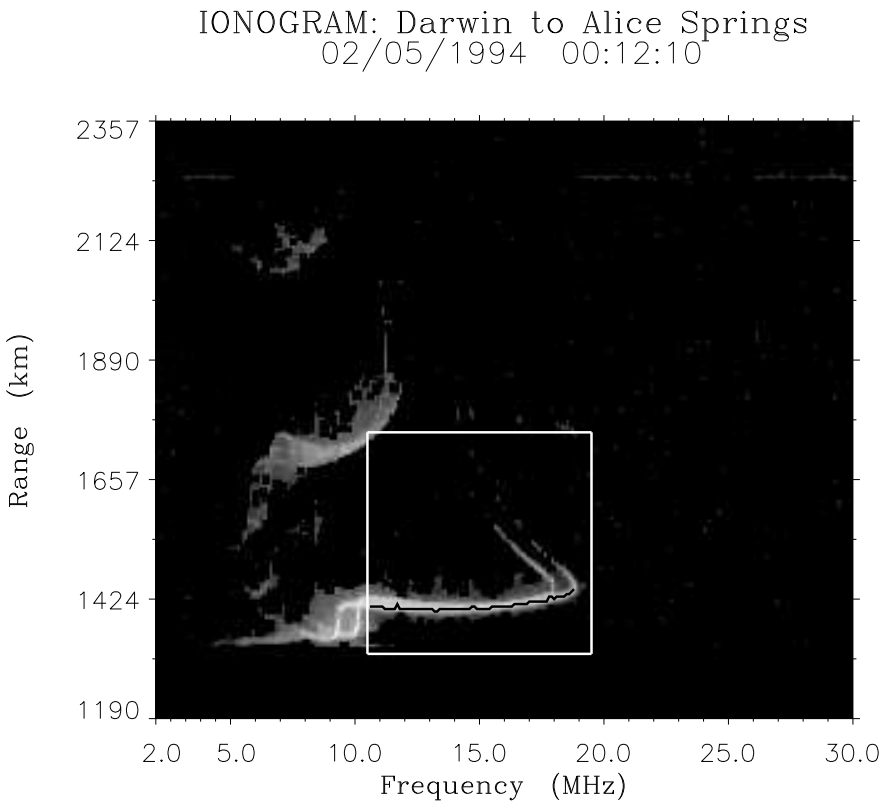

Figure 8: The ROF around one of the tracks. The ROF is represented by the white box overlaid upon the smoothed ionogram from Figure 5. The black line represents the trace approximation which can be seen to follow the trace quite well.

The preprocessing adopted is to further ridge-enhance the morphologically skeletonised ionogram using the algorithm from [18], and then to remove the lower-ray trace from the ROF, based on its approximation. Figure 10(a) shows the ROF preprocessed for the HT.

2.3.1 Mode separation

The FMS ionosonde provides no polarisation information. It is therefore necessary to separate the two modes of propagation, the *o*- and *x*-modes. Although the two polarization traces are related through some unknown complex relationship, this can be approximated (to first order) by a lateral shift in frequency. The lateral shift assumption holds around the nose of the trace particularly well. Furthermore the upper-ray traces are, for a significant length, straight lines.

A technique that can be used to search for lines in an image is the Hough transform, a parametric technique for detecting lines and shapes in binary images which, ideally, transforms global image features into a single peak representing the parameters of the feature. It is robust to uncorrelated noise and missing data, making it an appealing technique. Reviews of the Hough transform and its many generalisations can be found in Iannino and Shapiro [10], Illingworth and Kittler [9] and Leavers [14].

It is convenient to follow Duda and Hart [4] in using the normal form of the equation for a straight line,

namely

$$\rho = x\cos\theta + y\sin\theta, \tag{3}$$

where ρ is the normal distance to the line from the origin and θ is the angle between the normal and the x-axis. The straight line Equation 3 may be interpreted as a parametric transformation between an image space (x, y) and a parameter space or *Hough space* (ρ, θ). Any point in the image space can be transformed to a sinusoidal curve in the Hough space given by Equation 3. Conversely, a point (ρ, θ), in the Hough space uniquely describes a straight line in the image plane. Thus collinear points in the image, will be transformed to sinusoidal curves in the Hough space which intersect at a common point. The parameters of a line in the image can be found by finding this intersection.

When the image is discrete, each point in the image may be transformed and the resultant sinusoidal curve used to increment an accumulator array corresponding to a discrete version of the Hough space. Intersection points will be incremented more often and so the problem of straight line detection becomes one of finding a peak in the Hough space. In essence each point in the image *votes* for the lines it may be a part of and the most popular line *wins*.

The Hough transform has been adapted here to finding a pair of parallel straight lines simply by finding the maximum of a smoothed version of the Hough space and then searching the row of the Hough space for a second peak corresponding to a parallel line within the allowable ranges for the separation between the o- and x-modes, 0.4 to 1.2 MHz in this application. The Hough transform of the preprocessed ROF in Figure 10(a) can be seen in Figure 9. The smoothing is to remove the occurrence of spurious peaks in the Hough space. The lines corresponding to the two peaks in Figure 9 can be seen in Figure 10(b). This technique for finding the upper-ray traces does not rely on the upper-ray traces being linear, only on a significant segment of them being linear.

The computational cost of the Hough transform is drastically reduced by considering only the small ROF as suggested and removing most of the data points from this region. Thus a process which is normally very computationally intensive can be performed very quickly. In addition to this it can be further improved in speed by only considering a small angle range. In this application only lines with normal angles between 0 and 65 degrees were considered.

The major complication in applying the Hough transform arises because of the discrete nature of the image and the Hough space. The discrete nature of the image means that points are not truly collinear, while the discrete nature of the Hough space causes errors in the measurements of parameters. The resolution of the image cannot easily be altered but the resolution of the Hough space can be chosen. This choice is motivated by a tradeoff between computation speed and accuracy. Basically, the finer the accuracy, the more computation is required, though this is complicated by other factors as well (for instance see [**?**, 20]). In this application the resolution of the Hough space was chosen at 0.25 degrees by 0.5 pixels. This is convenient and provides sufficient accuracy as well as fast operation.

The two straight line approximations give the separation between the two modes, but in addition the o-mode line can be used as an approximation for the o-mode upper-ray trace. This approximation is used by considering the longest section of the o-mode line which coincides with the actual trace. This section is shown in Figure 10(c), along with the lower-ray trace approximation found through tracking.

The approximations for both upper- and lower-ray traces can now be used for the trace extraction by finding the minimum cost path between the two approximations' end points. This is done using an algorithm of Dijkstra [3] which finds least cost paths through networks of nodes, in this case the nodes being pixels which are connected to their eight neighbouring pixels.

The cost of traversing a pixel (or traversing a node in the network) must be carefully chosen for a particular problem. In this application a simple cost based on pixel brightness was used. Smoothing could be accomplished here by including some non-local element in the cost, but it seems that smoothing might be best accomplished as a post-processing step. An essential fact is that the cost function must vary non-linearly with pixels brightness if the curve is to be able to model a *sharp* nose shape, such as the F-layer trace,

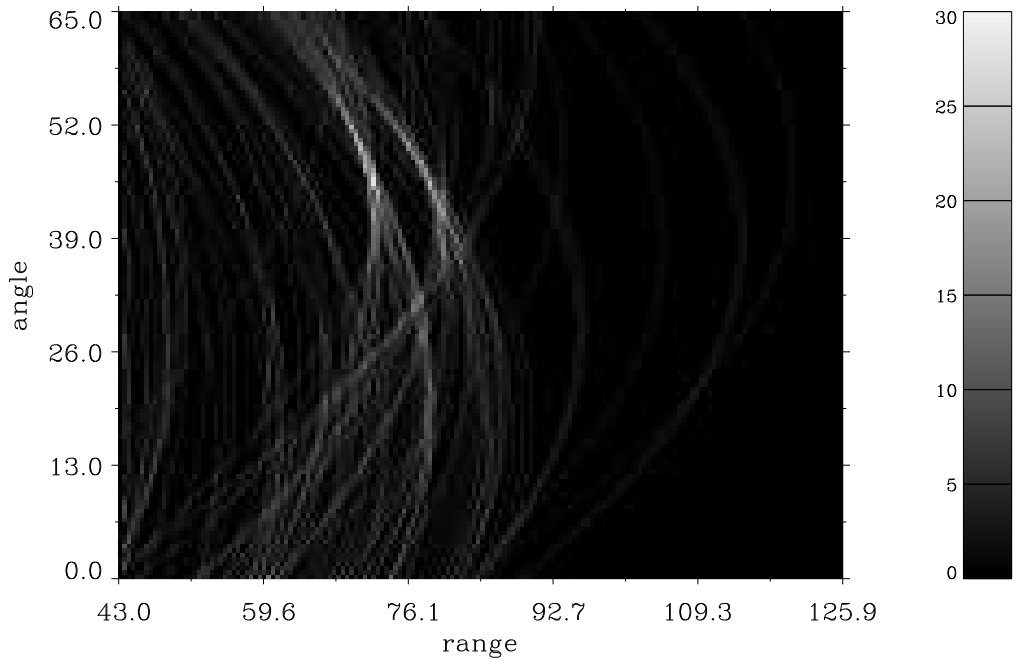

Figure 9: The Hough transform of the ROF in Figure 10(a). The scale shows the number of collinear points along a line of the specified parameters. The range is in pixels and angle in degrees. Two obvious peaks occur at almost the same angle.

without jumping between the upper- and lower-ray traces before reaching the nose. The non-linear function chosen here was the exponential function which is logical in this context because the ionogram displays log(power).

The path found through Dijkstra's algorithm is one of the final traces. Figure 10(c) shows the two end-points chosen for the example trace in Figure 8 and Figure 10(d) the trace found between them.

2.4 Classification

Once the traces in the ionogram have been extracted they must go through a final phase to select a single F2-layer trace, or decide that such a trace is not present in the image.

At present this is done by estimating the critical frequency of the o-mode F2-layer, f_oF2, using a horizontal profile of the ionogram. The critical frequency of the trace is the highest frequency which is reflected by the corresponding layer of the ionosphere. The estimate of f_oF2 found from the profile is relatively inaccurate but by choosing the longest extracted trace with a f_oF2 within 1.0 MHz of the estimate, the F2-layer trace is generally found. If no trace falls within 1.0 MHz of the estimate then the algorithm returns nothing.

In the example shown there was only one trace; which did meet the criterion, and it is shown in Figure 11.

Much better methods for performing classification than the heuristic rule used above could be found. For

instance with better statistical knowledge of the occurrence of the F2-layer trace, some kind of statistical classifier, based on position could be used. Another useful ideal is that of shape based classification is suggested as a method for performing classification. More work must be done on this phase of the algorithm.

3 Results

The algorithm was manually tested on 100 ionograms, with the results being classified into four categories:

Good: The algorithm picked the trace so that there was no significant difference between the automatically extracted trace, and one extracted by a person.

Acceptable: There was some small feature of the automatically extracted trace which did not match the real trace, but the output was still acceptable for use in an inversion program.

Unacceptable: The output was incorrect, and unsuitable for use in an inversion program.

No return: No trace was returned by the algorithm. The algorithm could not find a trace with a suitable level of confidence.

The number of ionograms falling into each category was 53, 9, 17 and 21 respectively.

It is worth noting that having no return for 21 of the ionograms was not unacceptable as approximately 15 were difficult to analyse by hand, and no F2-layer trace could confidently be found in these cases. The failure in 17 cases can be attributed to a number of causes, but in the majority of cases the failure was in final classification stage, showing that a more rigourous final classification needs to be adopted.

Such testing provides a qualitative assessment of the algorithms performance but it is desirable to have a quantitative measure with which to assess the algorithm. The ideal quantitative measure of performance would be to invert the trace and compare the resultant profile of the ionosphere with the real ionospheric profile, but this is not possible because real ionospheric profiles are not in general available.

The error in the critical frequency, f_oF2, of an automatically extracted trace forms a convenient measure of the accuracy of the trace. The critical frequency can be quickly extracted by hand from a large set of ionograms, and is one of the most important parameters of a trace, when used in inversion algorithms. Furthermore errors in f_oF2 has been used to asses trace extraction from vertical incidence ionograms in [5, 8, 17].

The measure is somewhat conservative, as in almost no cases will the error be small for an incorrectly extracted trace, but it may be significant even when the extracted trace is a good approximation to the real trace everywhere except near the nose of the trace.

Each ionogram was inspected by hand. As it is not always possible to select the critical frequency exactly, a range of critical frequencies was chosen for the F2-layer. The critical frequency of an automatically extracted trace was taken to be the frequency of the rightmost point of the trace. The error in critical frequency was taken to be the distance (in MHz) of the automatically extracted trace's critical frequency from the manually selected range of critical frequencies.

Approximately 1000 ionograms, recorded during days 168 to 197 of 1995, in support of the Jindalee over-the-horizon radar, were tested resulting in the histogram for the errors in critical frequency shown in Figure 12. This represents only one time period, and in the future tests will have to be conducted during other seasons, and stages of the solar cycle, but the results are expected to be at least as good, given that the current period of the solar cycle presents the most difficulties with respect to trace extraction because phenomena such as spread F are at their height.

Figure 13 shows the percentage cumulative absolute errors in the traces that were returned. As in the qualitative test the algorithm did not find traces in all cases. For approximately 30% of ionograms no trace was found. This is higher than the percentage of ionograms which are truly difficult to analyse and so some work remains in finding traces for the 10-15% of ionograms with a detectable F2-layer trace which the algorithm cannot currently extract.

The figures illustrate the algorithms performance well, demonstrating a error rate comparable to that for existing vertical incidence automatic trace extraction algorithms [5, 8, 17]. For instance approximately 73% of the traces found were in error by not more than than 0.1 MHz while approximately 10% of the traces found had absolute errors of greater than 0.5 MHz.

By comparison in [17] the manually estimated value of f_oF2 was compared directly with that calculated by their algorithm for extracting traces from vertical incidence ionograms, for 577 ionograms, with the result that 82% of traces were within 0.5 MHz of the manually estimated value. Thus, at least in this respect, the algorithm described herein is competitive, even though the algorithm of [17] operates on the easier vertical incidence ionograms, and incorporates information from hardware such as polarization mode. The added difficulty of the oblique problem is reflected in the fact that traces could be found for only 70% of ionograms as opposed to 100% in [17].

The computation time of the algorithm was important for the algorithm to be useful in providing real-time propagation advice. In its proposed use, an ionogram would be collected approximately every two minutes, but much of this time was to be used for other data processing tasks. The computation time allocated to trace extraction was 20 seconds on a DEC Alpha AXP, running Open VMS. The computation times of the algorithm for the set of 1000 ionograms were all between 2 and 16 seconds, with an average time of 11 seconds.

4 Conclusion

In conclusion there are several points to be made. Firstly, and most importantly, there is good evidence that the algorithm performs well. Section 3 displays an objective measure of the errors involved in running the algorithm on what has been presumed to be a fairly average set of data (though it is perhaps worse than average). Section 3 also provides other details of the results, and indicates some of the limitations of the algorithm. Further tests on larger sets of data are required before the algorithms performance can be assessed conclusively.

The algorithm is by no mean perfect as its error rate shows, but it is expected that more development will be done on it before a final version is included in the Jindalee over-the-horizon radar system. More work is required on the latter stages of the algorithm, for instance, the final classification stage. Also the algorithm is limited in that it cannot perform well in cases where a *series* of ionograms provides crucial data, such as the case when sporadic E blankets the F-layer.

Another point worth mentioning is that the FMS set of ionograms have only one possible baseline. Ideally an algorithm could be found that would work for any transmitter/receiver pair. Some work has been done towards generalising the algorithm documented herein to different sets of ionogram, with very promising results.

The principle advantage of the algorithm is that it is non-parametric and thus does not require an ionospheric model to work; the only models for oblique propagation being intractably complex. Being non-parametric also has the benefit of allowing more generality than most parametric systems would allow. For instance the algorithm can capture the sometimes quite complex shape of the F-layer trace when a TID passes through the layer.

Finally, it is worth reiterating that this work has been directed towards automatic trace extraction of the

o-mode F2-layer trace, though the method is generic enough to find other layers when they are present. If multiple hop traces become important then with some adaption the algorithm could be used to find these layers.

Acknowledgement

This work was supported by the High Frequency Radar Division of The Defence Science and Technology Organisation of Australia. The author would like to Dr Steve Brown for the use of code to perform Dijkstra's algorithm and Dr John Percival for many helpful discussion and comments.

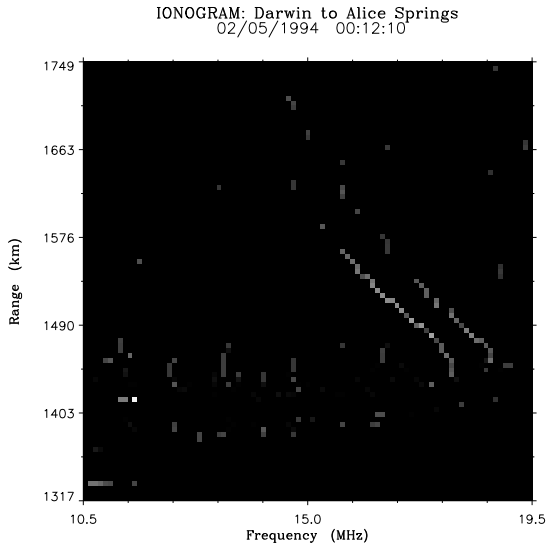

(a) The ROF from Figure 8, preprocessed to be used in the Hough transform for mode separation.

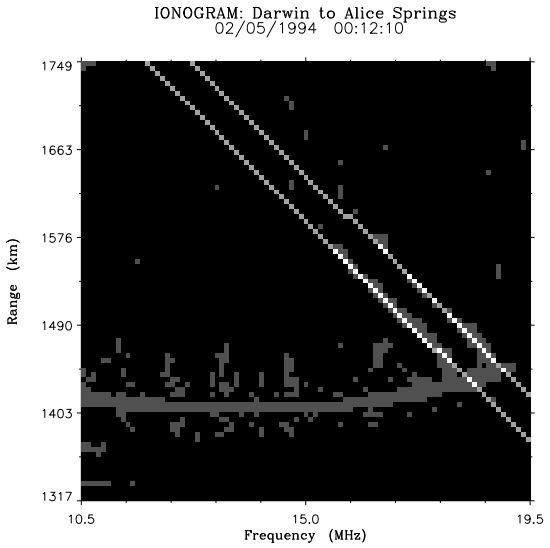

(b) The pair of lines corresponding to the pair of peaks in the HT shown in Figure 9.

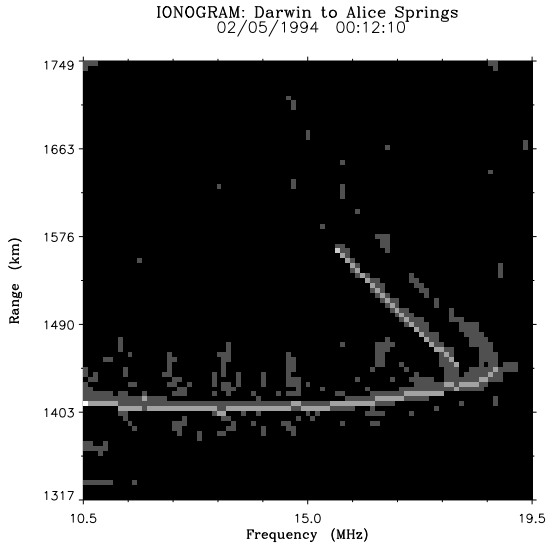

(c) The approximations for the upper- and lower-ray traces and their end points.

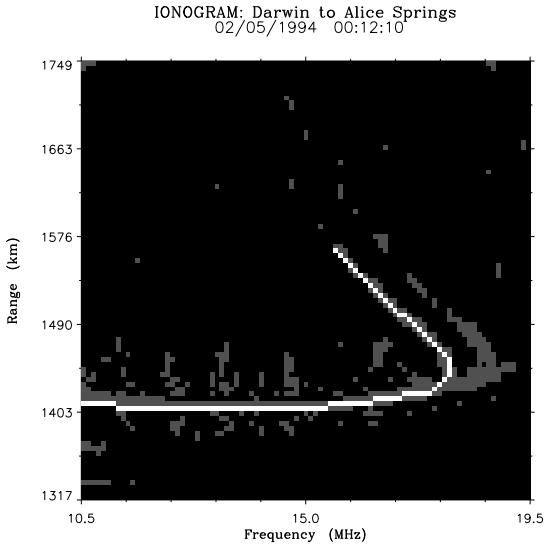

(d) The result of the cost minimisation method for finding the trace.

Figure 10:

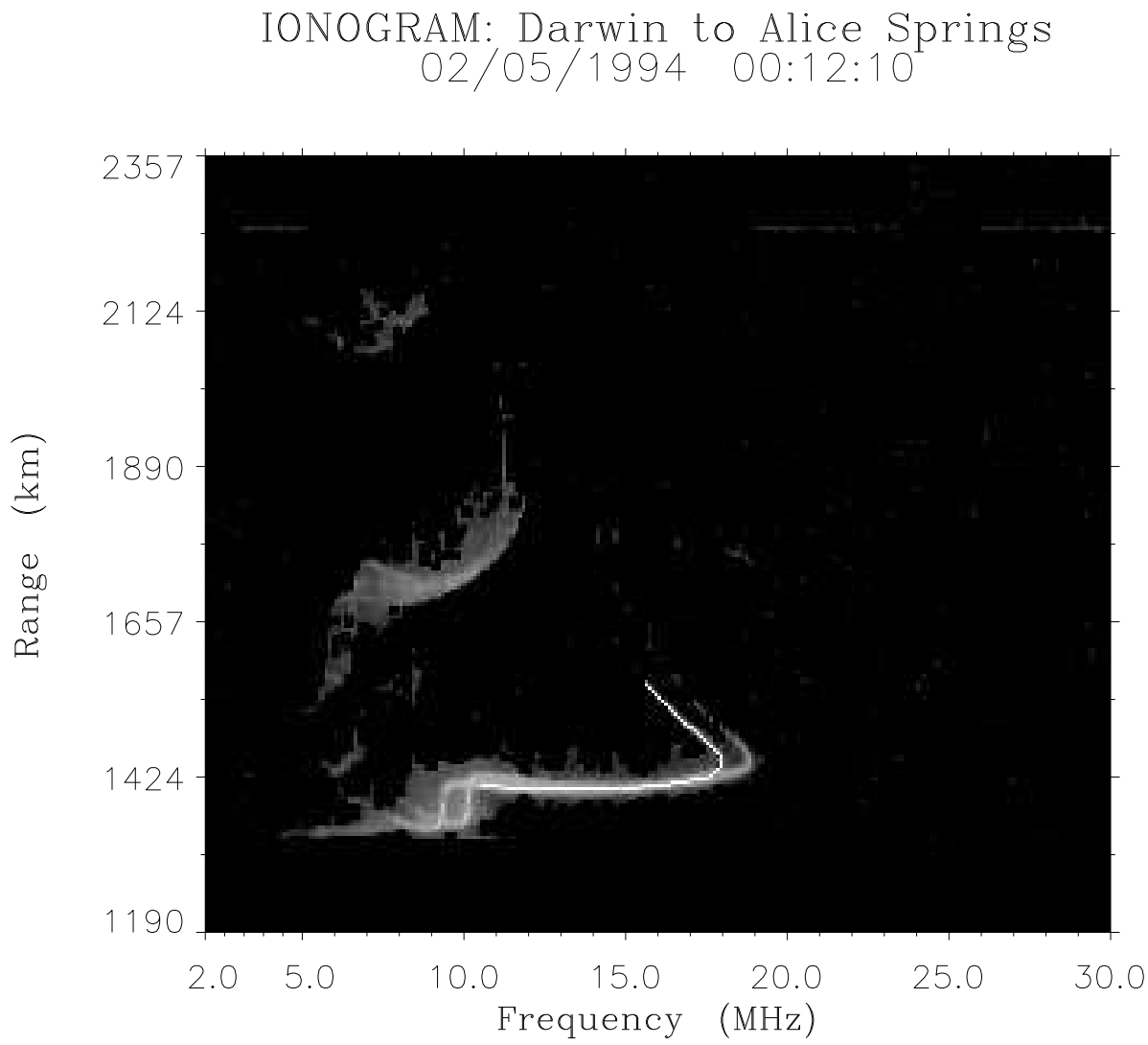

Figure 11: The F2 layer trace found by the ionogram overlaid on the smoothed ionogram.

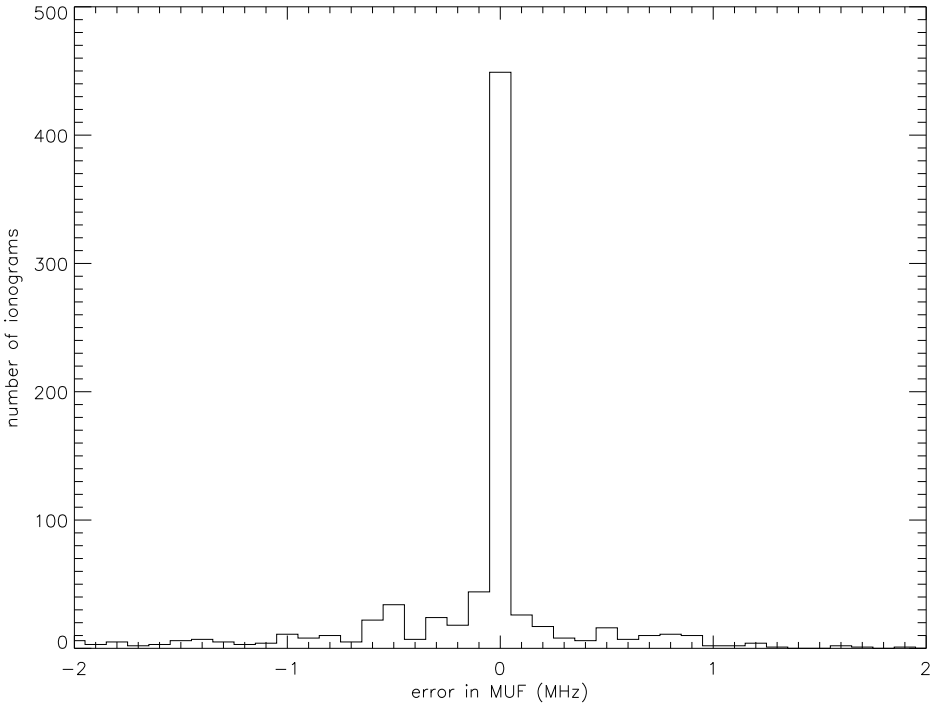

Figure 12: A histogram for the errors in the critical frequency of the *o*-mode F2-layer trace.

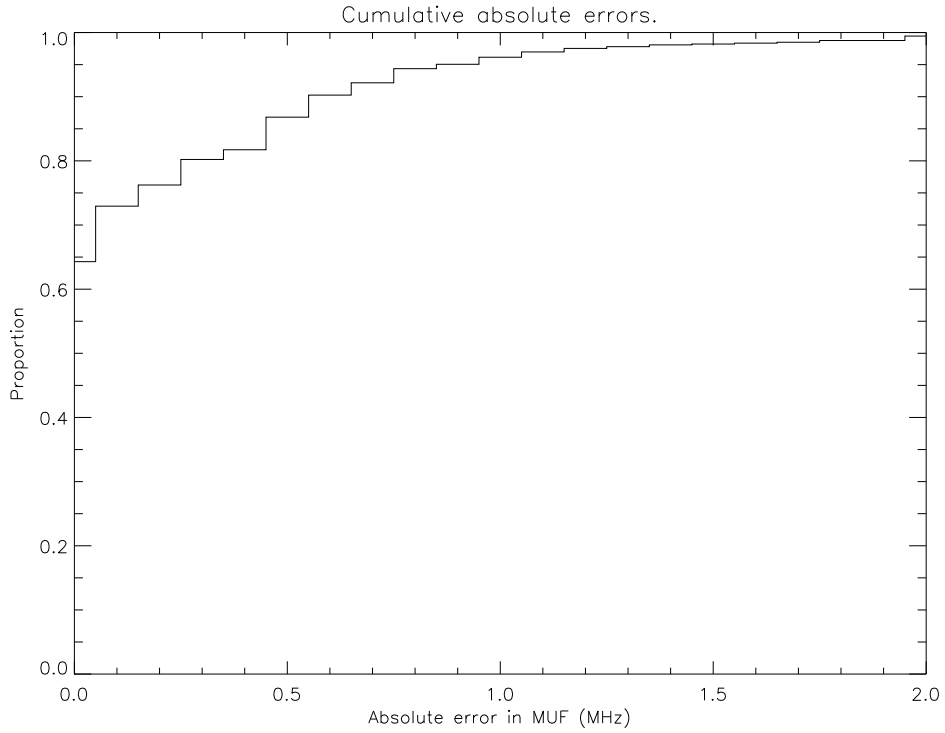

Figure 13: A cumulative histogram for the absolute errors in the critical frequency of the *o*-mode F2-layer trace.

References

[1] G.F. Earl andd B.D. Ward. *Radio Science*, **22**, pp 275–291, 1987.

[2] K. Davies. *Ionospheric Radio*. Peregrinus on behalf of the Institution of Electrical Engineers, 1990.

[3] E.W. Dijkstra. A note on two problems in connexion with graphs. *Numerische Mathematik*, **1**, pp 269–271, 1959.

[4] R.O. Duda and P.E. Hart. Use of the Hough transform to detect lines and curves in pictures. *Communications of the ACM*, **15**, 1, pp 11–15, 1972.

[5] J.D. Gilbert and R.W. Smith. A comparison between the automatic ionogram scaling system and the standard manual method. *Radio Science*, **23**, 6, pp 968–974, 1988.

[6] R.M. Haralick and L.G. Shapiro. *Computer and Robot Vision*. Addison-Wesley Publishing Company, 1993.

[7] J. Hazelwood. The application of attributed relational graphs to the problem of automatically scaling oblique ionograms. Master's thesis, University of Lowell, 1992.

[8] S. Igi, H. Minakoshi, and M. Yoshida. Automatic ionogram processing system 2. automatic ionogram scaling. *Journal of the Communications Research Laboratory*, **39**, 2, pp 367–379, 1992.

[9] J. Illingworth and J. Kittler. A survey of the Hough transform. *Computer Vision, Graphics, and Image Processing*, **44**, pp 87–116, 1988.

[10] A. Inannino and S.D. Shapiro. A survey of the Hough transform and its extensions for curve detection. *Proc. IEEE Comput. Soc. Conf. Pattern Recognition and Image Processing*, pp 32–38, 1978.

[11] R. Kasturi and R.C. Jain. *Computer Vision*: Principles. IEEE Computer Society Press, 1991.

[12] T.H. Koschmieder. A neural network to identify stray signals in ionograms. *Radio Science*, **29**, 6, pp 1467–1471, 1994.

[13] I.V. Krasheninnikov and B.E. Liannoy. Estimation of the true ionospheric height profile, with a continuous gradient, from oblique sounding data. *Journal of atmospheric and terrestrial physics*, **52**, 2, pp 113–117, 1990.

[14] V.F. Leavers. *Shape Detection in Computer Vision Using the Hough Transform*. Springer-Verlag, 1992.

[15] P. Maragos and R.B. Ziff. Threshold superposition in morphological image analysis systems. *IEEE Transactions on Pattern Recognition and Machine Intelligence*, **12**, 5, pp 498–504, 1990.

[16] M.H. Reilly and J.D. Kolesar. A method for real height analysis of oblique ionograms. *Radio Science*, **24**, 4, pp 575–583, 1989.

[17] B.W. Reinisch and H. Xueqin. Automatic calculation of electron density profiles from digital ionograms 3. processing of bottomside ionograms. *Radio Science*, **18**, 3, pp 477–492, 1983.

[18] M. Roughan. A method for generalising binary skeletonisation algorithms to gray-scale images. *in submission*.

[19] H.W. Sorenson, editor. *Kalman Filtering: Theory and Application*. IEEE Press, 1985.

[20] K.S.Y. Yuen W.C.Y. Lam, L.T.S. Lam and D.N.K. Leung. An analysis on quantizing the Hough space. *Pattern Recognition Letters*, **15**, pp 1127–1135, 1994.